LINK TO ORIGINAL ARTICLE

Imaging hippocampal subregions with *in vivo* MRI: advances and limitations

Niels M. van Strien, Marius Widerøe, Wilma D. J. van de Berg and Harry B. M. Uylings

In their recent Review article (A pathophysiological framework of hippocampal dysfunction in ageing and disease. *Nature Rev. Neurosci.* **12**, 585–601 (2011))[1], Small *et al.* present a compelling framework for differentiating hippocampal disorders based on the selective vulnerability of hippocampal subregions using recent neuroimaging findings. This framework stimulates thoughts about how (dys)function of distinct hippocampal subregions relates to disease and how it can be assessed in the future using high-resolution structural and functional MRI. The impact this pathophysiological framework has on clinical practice depends to a great extent on the availability, quality and reliability of methods to discern hippocampal subregions *in vivo*. In many hospitals, 3-Tesla MRI scanners have become the standard for obtaining high-resolution *in vivo* brain images, and the introduction of 7-Tesla MRI may lead to a revolutionary increase in image detail. Nonetheless, accurately measuring hippocampal subregions with *in vivo* MRI has proved to be challenging[2]. In this Correspondence, we illustrate how human *in vivo* MRI acquisition and image post-processing methods need to advance to reliably measure and differentiate hippocampal subregions.

In neuroanatomy, hippocampal subregions are discerned on the basis of transitions in cytoarchitecture[3] (such as the number of

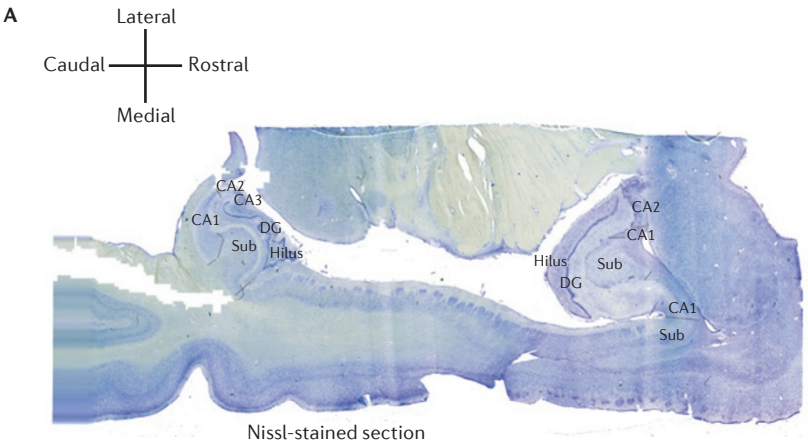

Figure 1 | **Histology, *ex vivo* and *in vivo* MRI of the human hippocampus. A** | 50 µm thick Nissl-stained oblique horizontal section. **Ba** | Same tissue as **A** at a similar angle, T_1-weighted image at 7 Tesla (resolution: 0.25 mm isotropic voxels; acquisition time: 30 h, 15 min). The red line shows the plane of the cross section shown in **Bb**. **Bb** | Oblique coronal image. **C** | Coronal T_2-weighted image of the Penn hippocampus atlas[10] measured at 9.4 Tesla (resolution: 0.2 mm isotropic voxels; acquisition time: 62.5 h). **D** | Oblique coronal T_2-weighted image measured at 3 Tesla *in vivo*; same subject as **E** at approximately the same level (resolution: 0.75 mm in-plane; slice thickness 0.8 mm; acquisition time: 18 min). The hippocampal formation is located in the red circles. **E** | Oblique coronal image measured with 3-Tesla *in vivo* functional MRI; same subject as **D** (resolution: 1.5 mm in-plane; slice thickness 3.0 mm; acquisition time per volume: 2.0 s). DG, dentate gyrus; Sub, subiculum.

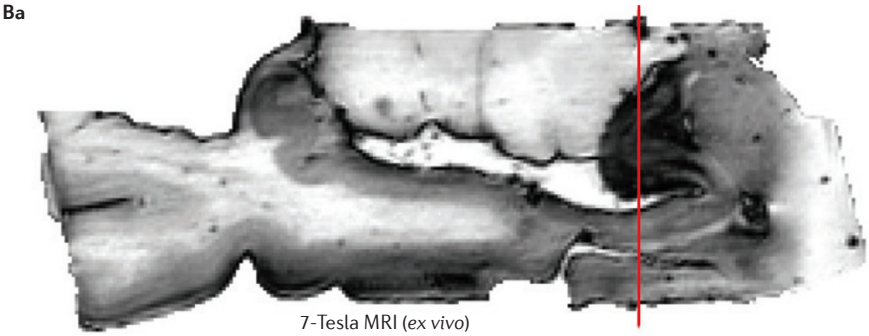

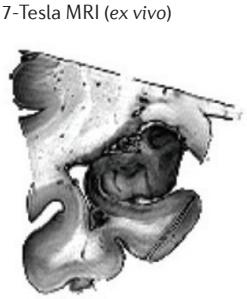

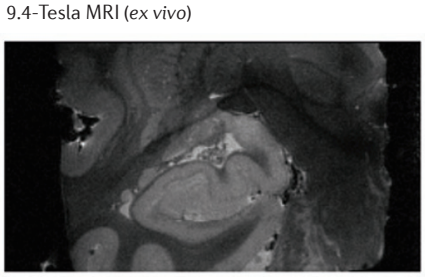

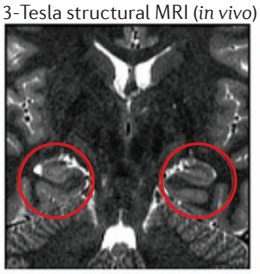

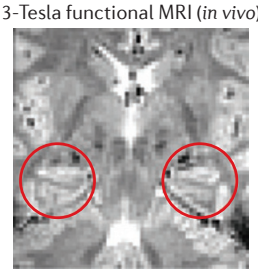

cortical layers or the density of a cell layer) that can be made visible in, for example, Nissl-stained tissue (FIG. 1A). Using high-field-strength *ex vivo* MRI on small hippocampus samples, images that approach microscopic quality (for example, 0.1 mm isotropic voxels) can be obtained[4,5]. However, even then, the level of spatial detail is often too limited to reliably discern hippocampal subregions (FIG. 1B,C). This is even more challenging with *in vivo* 3- and 7-Tesla images. With a spatial resolution of 1.5 mm isotropic voxels in functional MRI images and more than 0.4 mm in structural images (FIG. 1D,E), the size of the smallest measuring unit (voxel) substantially exceeds the thickness of a cortical layer, resulting in an inability to reliably see cortical layers or layer transitions in such images.

In current *in vivo* neuroimaging studies in which hippocampal subfields are discerned, either a manual or automated segmentation procedure is applied that is based on visual or calculated similarity between the obtained magnetic resonance image and a detailed anatomical atlas of the hippocampal subdivisions. However, no reliable, quantifiable relationship between macroscopic anatomical landmarks (for example, folding patterns of gyri) and the exact location of hippocampal subregions is known to exist[6], despite reports that in other cortical regions, macroscopic features can be predictive for the underlying cytoarchitecture[7]. In healthy individuals, a probabilistic atlas may be used to determine the probability of the location of hippocampal subregions[8]. However, this atlas is based on healthy individuals and is likely to be invalid for determining subregions in individuals suffering from hippocampus-related pathology, as the pathology distorts the geometry of the hippocampal subregions differentially[9]. The Review by Small *et al.* provides an excellent starting point to advance knowledge about the relationship between high-resolution *in vivo* and *ex vivo* MRI and histopathological images, yet clinical relevance will only increase if methods that allow accurate localization of hippocampal subfields using *in vivo* MRI become available.

Niels M. van Strien and Marius Widerøe are at the Department of Circulation and Medical Imaging, Faculty of Medicine, Norwegian University of Science and Technology, Trondheim, Norway.

Wilma D. J. van de Berg and Harry B. M. Uylings are at the Department of Anatomy and Neurosciences, Neuroscience Campus Amsterdam, VU University Medical Center, Amsterdam, The Netherlands.

Correspondence to N.M.v.S.
e-mail: niels.v.strien@ntnu.no

doi:10.1038/nrn3085-c1

1. Small, S. A. *et al.* A pathophysiological framework of hippocampal dysfunction in ageing and disease. *Nature Rev. Neurosci.* **12**, 585–601 (2011).
2. Olman, C. A., Davachi, L. & Inati, S. Distortion and signal loss in medial temporal lobe. *PloS ONE* **4**, e8160 (2009).
3. Rosene, D. L. & Van Hoesen, G. W. in *Cerebral Cortex* Vol. 6 (eds Jones, E. G. & Peters, A.) 345–455 (Plenum Publishers, New York,1987).
4. Fischl, B. *et al.* Predicting the location of entorhinal cortex from MRI. *Neuroimage* **47**, 8–17 (2009).
5. Fatterpekar, G. M. *et al.* Cytoarchitecture of the human cerebral cortex: MR microscopy of excised specimens at 9.4 Tesla. *Am. J. Neuroradiol.* **23**, 1313–1321 (2002).
6. Amunts, K. *et al.* Cytoarchitectonic mapping of the human amygdala, hippocampal region and entorhinal cortex: intersubject variability and probability maps. *Anat. Embryol.* **210**, 343–352 (2005).
7. Fischl, B. *et al.* Cortical folding patterns and predicting cytoarchitecture. *Cereb. Cortex* **18**, 1973–1980 (2008).
8. Eickhoff, S. B. *et al.* A new SPM toolbox for combining probabilistic cytoarchitectonic maps and functional imaging data. *Neuroimage* **25**, 1325–1335 (2005).
9. Van Hoesen, G. W. & Hyman, B. T. Hippocampal formation: anatomy and the patterns of pathology in Alzheimer's disease. *Prog. Brain* Res. **83**, 445–457 (1990).
10. Yushkevich, P. A. *et al.* A high-resolution computational atlas of the human hippocampus from postmortem magnetic resonance imaging at 9.4 T. *Neuroimage* **44**, 385–398 (2009).

Acknowledgements
N.M.v.S was supported by the Norwegian Research Council (Independent projects – Biology and Biomedicine grant number 197245).

Competing interests statement
The authors declare no competing financial interests.

FURTHER INFORMATION
Niels M. van Strien's homepage:
http://www.temporal-lobe.com

ALL LINKS ARE ACTIVE IN THE ONLINE PDF